

General Disclaimer

One or more of the Following Statements may affect this Document

- This document has been reproduced from the best copy furnished by the organizational source. It is being released in the interest of making available as much information as possible.
- This document may contain data, which exceeds the sheet parameters. It was furnished in this condition by the organizational source and is the best copy available.
- This document may contain tone-on-tone or color graphs, charts and/or pictures, which have been reproduced in black and white.
- This document is paginated as submitted by the original source.
- Portions of this document are not fully legible due to the historical nature of some of the material. However, it is the best reproduction available from the original submission.

NASA Technical Memorandum 79072

(NASA-TM-79072) EVALUATION OF TWO INFLOW
CONTROL DEVICES FOR FLIGHT SIMULATION OF FAN
NOISE USING A JT15D ENGINE (NASA) 17 p HC
A02/MF A01 CACL 21E

N79-15969

Unclas

G3/07 43645

EVALUATION OF TWO INFLOW CONTROL
DEVICES FOR FLIGHT SIMULATION OF
FAN NOISE USING A JT15D ENGINE



W. L. Jones, J. G. McArdle, and L. Homyak
Lewis Research Center
Cleveland, Ohio

TECHNICAL PAPER to be presented at the
Fifth Aeroacoustics Conference
sponsored by the American Institute of Aeronautics and Astronautics
Seattle, Washington, March 12-14, 1979

EVALUATION OF TWO INFLOW CONTROL DEVICES FOR FLIGHT SIMULATION OF FAN NOISE USING A JT15D ENGINE

W. L. Jones, J. G. McArdle, and L. Homyak
NASA Lewis Research Center
21000 Brookpark Road
Cleveland, Ohio 44135

Abstract

Two inflow control devices, (ICD's) one in-duct and the other external to the duct were tested on a JT15D engine to determine their ability to remove inflow turbulence without altering the sound transmission to the far field. The objective of the program was to develop means of accurately simulating flight fan noise on ground static test stands. The results generally indicated that both the in-duct and external ICD's were effective in reducing the inflow turbulence and the fan blade passing frequency tone generated by the turbulence. The external ICD was essentially transparent to the propagating fan tone but the in-duct ICD caused attenuation under most conditions.

Introduction

The simulation of in-flight turbofan engine noise using ground static test facilities requires the use of inflow control devices to provide clean inflow and acoustic signatures characteristic of the engine in flight.¹ Inflow disturbances on ground static test stands arise from atmospheric turbulence, ground vortices or eddies from test stand structure.² These disturbances have been shown to produce added noise from turbofan engine fans that incorporate advanced noise reduction design features.³ In the present investigation two inflow control devices (ICD's) were tested to determine their suitability for providing flight-like inflow to the engine and also to determine any possible noise attenuation and changes in directivity caused by their use. The engine used for this investigation was a P&W JT15D turbofan engine. Two types of ICD's were used in the investigation. The first was external to the duct⁴ and the second an internal duct type.⁵ The program results reported herein are a part of a larger planned inter-center forward velocity effects program utilizing the JT15D engine in flight, static, and wind tunnel tests.

A method of calibration of the ICD's transmission characteristics was devised which involved the use of rods mounted in the inlet duct a short distance (3.5 in.) upstream from the fan. Two rod configurations were utilized for the calibration. The first configuration utilized 28 rods and the second, 41 rods. The rod configurations were designed to generate different modal patterns in the inlet duct.^{6,7} These modal patterns produce definite BPF tone directivity patterns in the far field⁸ that are distinct from the no rod case. The intensity of the BPF tone source noise generated by the fan blades cutting the rod wakes also was intended to be sufficiently high to completely dominate over the noise generated by the interaction of the fan rotor blades with the inflow turbulence. Thus it was intended to generate a tone whose source would not be affected by the presence of the ICD's. By use of different rod configurations it was possible to determine the transmission characteristics over a range of duct sound modal structures whose effect could be identified in the far field.

Apparatus and Procedure

Engine

The engine used in this investigation was a Pratt & Whitney JT15D. This turbofan engine has a bypass ratio of 3.3, a fan pressure ratio of 1.5, and a maximum rated thrust of 9800 newtons (2200 lb). Fig. 1 presents a cross section view of the JT15D engine and indicates instrumentation station locations. The core engine consists of a single stage centrifugal compressor driven by a single stage axial turbine. The fan is directly driven by a two stage axial turbine. The fan has 28 blades and is 0.534 m (21 in.) in diameter. There are 66 fan bypass stator vanes and 33 core stator vanes. The fan to fan stator spacing is about 1.0 fan blade cord and the fan to core stator spacing is about 0.3 fan blade cord. The blade-vane ratio for this fan lead to a cut-off rotor-stator interaction tone for the fan and bypass stator vanes. The tone due to interaction between fan and core stator vanes, however, was "cut-on" for all engine speeds. Thus considering also the close spacing, tones due to rotor wakes interacting with the core stators are a strong possibility in the JT15D production engine.

Test Facility

The Lewis outdoor test facility for noise and performance testing can accommodate turbofan engines with thrust levels up to 133 500 newtons (30 000 lb). A perspective sketch of this facility is shown in Fig. 2. The engine is supported by a tripod, cantilevered, overhead support arm. The support arm contains a thrust measuring system to which the engine is mounted. The centerline engine height above the ground is 2.9 m (9.5 ft). A movable shelter, on tracks, is used to provide a work area and to protect the engine between runs.

The JT15D engine is shown mounted on the test stand in Fig. 3. The engine is mounted on a pylon support arm which permits the air inlet to be forward of the major overhead support system. This arrangement helps minimize the possibility of inlet flow distortions caused by wakes and eddies from flow over the test stand structure. Fig. 3 also shows the engine connected to an exhaust muffler. Aft-radiated engine as well as jet noise was effectively eliminated by the use of this muffler.

Acoustic Instrumentation and Processing

Far field noise measurements were made with microphones located on a 27.4 m (90 ft) radius arc centered on the engine inlet. The microphones were positioned at 10° intervals from 0° to 120°. The majority of the acoustic measurements were made with ground microphones. These microphones 1.3 cm (0.5 in.) diameter were mounted on 0.6 m (2 ft) square composition hard board at ground level and

pointed at the engine inlet. Some measurements were also made with engine centerline height microphones mounted to pole stands and pointed toward the engine inlet. In addition in-duct Kulite transducers mounted about 30.5 cm (12 in.) upstream of the fan were also utilized (Fig. 1). The microphone signals were transmitted over shielded cable and were recorded on FM tape and analyzed through a Novatronic scanner control unit. The Novatronic separately plays each acoustic channel into a General Radio multifilter and multichannel RMS detector. Using a 8-second integration time, one-third octave band sound pressure level (SPL) was obtained. Integration was performed over 1024 data samples to reduce uncertainty of the random signal measurement. The resulting sound pressure levels, in units of decibel (dB), are referenced to 2×10^{-5} pascals (0.002 microbar). All further data was processed on an IBM-360 computer.

The IBM computer calculated sound levels at distances other than the measurement stations⁹ and corrects the data to an atmospheric temperature of 15° C (59° F) and a relative humidity of 70 percent. Ground microphone data are corrected to free-field conditions by subtracting 6 dB at all frequencies up to 20 000 Hz. This correction accounts for the effect of ground reflected signals.

Inflow Control Devices

Two inflow control devices (ICD's) were used in the investigation. The external type is shown mounted on the engine in Fig. 4. The internal duct type is shown in Fig. 5 installed in the engine inlet duct. A schematic diagram of the two ICD types is shown in Fig. 6. Honeycomb cell size and thickness are given for both the external and internal duct ICD's. Four in-duct ICD honeycomb configurations consisting of three thicknesses and two cell sizes were tested. Only the results of the 4 inch thick 3/8 inch cell size configuration are reported in this paper.

The external ICD (hereafter called ICD number 1) was designed to fit snugly around the engine nacelle and was positioned axially for alignment of the honeycomb cells with the potential flow streamlines for the inlet. The design through flow velocity for the in-duct ICD (hereafter called ICD number 2) was approximately 400 ft/sec at maximum engine flow. Through flow velocity for the external ICD was 15 ft/sec.

Test Procedure

The engine was run over a range of fan speeds from 6750 rpm to 15 000 rpm. The majority of the data, however are presented at 10 500 rpm and 13 500 rpm. These fan speeds correspond to a subsonic and a supersonic fan tip speed condition. Both aerodynamic performance data and acoustic data runs were made on each configuration. Baseline acoustic data runs were generally repeated on several days and then averaged to improve the data accuracy. The acoustic runs with the ICD's produced data that had considerably less scatter and was repeatable from one day to another.

All tests were performed when ambient wind speeds were less than 8.7 knots/hr (10 mph). Tests were generally performed with and without the ICD's on the same day to improve accuracy of data. AI-

though four different in duct ICD's were tested in the program only the 10.15 cm (4 in.) thick, 0.952 cm (3/8 in.) cell size honeycomb results are presented herein.

Results and Discussion

The results of a performance evaluation of two types of ICD's using the JT15D engine are reported. This evaluation was part of a larger forward velocity program involving flight testing, tunnel testing, and anechoic chamber testing of the JT15D engine or its fan stage. The performance evaluation of the two ICD's consisted of both changes in fan noise generation and possible noise transmission effects attributed to the ICD's.

The discussion of the results of the investigation is divided into noise generation and noise transmission effects. All runs were made with the aft end of the engine connected to an exhaust muffler, thus the data are for forward radiated noise only. The data is presented on a 1/3 octave band basis. Narrow band spectra are also presented for some of the comparisons.

Noise Generation Effects

The ICD's are intended to reduce engine inflow turbulence from the atmosphere and any wakes or vortices from either test stand structure or the ground plane. These disturbances can generate fan BPF tone noise as well as broadband and possibly other shaft order tones. Ideally, the ICD should condition the engine inflow to the extent that both the inflow and the resultant noise generated simulate the flight case. The extent to which flight-like noise generation was achieved by the types of ICD's used in this investigation is illustrated by examining Figs. 7 to 13. Fig. 7 presents the acoustic far field power spectra for the two ICD's as well as the baseline no ICD case. The 10 500 rpm fan speed condition is shown in Fig. 7(a). The BPF fundamental tone was reduced about 7 dB for either ICD. The second harmonic of this tone was reduced about 4 dB with ICD number 1 and about 8 dB with ICD number 2. Although the fan and bypass stators on the production JT15D engine used in this investigation are designed for acoustical cut-off of the BPF tone at 10 500 rpm, the fan and core stators do not have the required blade to vane ratio for cut-off. Therefore it is not certain whether the residual BPF tone with the ICD's is a result of insufficiently removed inflow turbulence or rotor/core stator interaction.

Fig. 7(b) presents the power spectrum for the 13 500 rpm condition again for the two ICD's. At this speed the BPF tone due to the rotor alone caused by supersonic fan blade tip speed can propagate. The inflow turbulence is not expected to greatly affect the BPF tone at supersonic blade tip speed. This supersonic condition also generates other multiple pure tones (MPT's) which dominate in the 3000 to 5000 Hz band. The data for ICD number 1 indicate very little change over the baseline case. The data using ICD number 2, however, show a reduction in acoustic far field power level for all frequencies above 500 Hz.

Narrow band spectra of far field noise at 60° from the inlet axis for a fan speed of 10 500 are

compared with and without ICD number 1 in Fig. 8. The dominant BPF tone is reduced considerably by the ICD (compare Figs. 8(a) and (b)). The higher harmonics of the BPF tones are also reduced significantly by the ICD. Narrow band in-duct data (measured by Kulite transducers mounted in the duct wall upstream of the fan) are shown in Fig. 9. The in-duct BPF tone and the second harmonic were reduced more than 10 dB by the ICD. Unsteadiness of the BPF tone is shown in Fig. 10. Fig. 10(a) illustrates the case without the ICD and Fig. 10(b) with the ICD. The effect of the ICD is to greatly reduce the unsteadiness of the tone.

Far field directivity of the BPF tone for both ICD's at 10 500 rpm is shown in Fig. 11(a). The data indicates very little difference between the two ICD's (except at the 40° and 80° angles). The data indicate that the tone reduction with the ICD's generally increases with angle from the inlet. The BPF tone directivity at 13 500 rpm is shown in Fig. 11(b). At low angles to the inlet both ICD's reduced the BPF tone noise of the fan however, at angles of 60° and greater ICD number 1 did not reduce the BPF tone noise level from that of the baseline. A possible explanation for this result is that, at low angles to the inlet, rotor turbulence dominates the noise generation and both ICD's are able to reduce this source while at angles of 60° and greater, the rotor alone field, due to supersonic tip speed, dominates the noise generation. This observation however does not completely explain ICD number 2 results at high angles. Apparently the rotor alone modal patterns generated by the fan and appearing at these angles are attenuated by the in-duct ICD in propagating to the far field. This behavior may be related, somehow, to the shock like nature of the rotor alone field at supersonic fan speeds. In the case of the BPF tone directivity at 10 500 rpm Fig. 11(a) (subsonic blade tip speed) the noise generated is primarily due to rotor turbulence which both ICD's are able to considerably reduce. The noise generated by the turbulence does not appear to be attenuated by ICD number 2 as was the case at the higher tip speed case (Fig. 11(b)).

The noise generated by the fan as measured in-duct at the two speed conditions and for the two ICD's is illustrated in Fig. 12. The data presented here was obtained from in-duct wall microphones and thus is an indication of the fan generated noise near the source. Fig. 12(a) presents 1/3 octave sound pressure level (SPL) spectra at 10 500 rpm fan speed. The data indicate that both ICD's were effective in reducing the BPF tone and the higher harmonics of the BPF. This result is in general agreement with the far field results for this speed (Fig. 7(a)). Fig. 12(b) presents data for the 13 500 rpm case. This data indicate that both ICD's reduced the generated fan noise slightly but the far field results (Fig. 7(b)) show a substantial reduction for ICD number 2. The far field result would seem to indicate that the in-duct ICD attenuated the propagating noise at supersonic fan tip speed while ICD number 1 did not.

The second harmonic tone directivity for the two ICD's is shown in Fig. 13. Fig. 13(a) presents the far field data at 10 500 rpm. Unlike the fundamental tone at this fan speed, the second harmonic tone due to rotor-stator interaction is

cut on. The data indicate that even though the noise source is cut on a reduction of inflow turbulence by the ICD's can reduce the noise level. The fact that ICD number 2 reduced the noise more than ICD number 1 may have been due to attenuation. The explanation for the behavior observed in Fig. 13(b) at the 13 500 rpm condition is similar to that for the fundamental tone at this speed.

Transmission Effects

As stated earlier a method of calibrating the ICD's for possible changes in far field directivity and or noise attenuation was devised that utilized wake generating rods mounted upstream of the fan. The rods were inserted through the duct wall 10.3 cm (3.5 in.) upstream of the fan (Fig. 14). Two rod configurations were utilized in the ICD calibration tests. The first configuration consisted of (28) 0.635 cm (1/4 in.) diameter rods and the second (41) 0.475 cm (3/16 in.) diameter rods. The rod numbers were chosen to interact with the 28 blades of the rotor to generate a strong BPF tone that would produce predictable in-duct modes and thus predictable far-field directivity characteristics.⁸ The 28 rod configuration produced highly propagating plane and axi-symmetric interaction modes within the engine inlet. The 41 rod configuration generated only one circumferential order ($m = 13$) of spinning modes that vary from near cut-off at low speeds to more highly propagating at higher speeds. The predicted far-field directivity for these known source modes was then used to determine the transmission characteristics of the ICD's. The BPF tone generated by the rods is not expected to be affected by the ICD's therefore any change in the far field noise level or directivity could be attributed to the ICD transmission characteristics.

The far field tone noise directivities for the 28 rod configuration at 10 500 rpm and 13 500 rpm are shown in Fig. 15. As mentioned previously the combination of rods and fan blades produces a BPF tone that consists primarily of a plane wave and axisymmetric modes that are highly propagating and thus beam the acoustic energy to the far field near or on engine axis. This result is illustrated by the large increase in SPL at the low directivity angles with the rods installed. At angles away from the axis the tone is dominated subsonically by the rotor-turbulence or rotor core stator interaction and supersonically by the rotor alone field. The 28 rod method of generating a calibration tone is useful only at small angles to the inlet axis.

The far field tone directivity for the 41 rod configuration is shown in Fig. 16. The directivity pattern generated by the rods generally exhibits the expected characteristic pattern, namely that the pattern is directed more away from the inlet than the 28 rod configuration, and the leading edge of the pattern advances to lower angles as engine speed increases.⁸ The rotor alone field can again be seen to appear at supersonic tip speed and to be dominate at the high angles. This type of directivity pattern should allow ICD calibration over a wider range of angles away from the inlet.

The transmission characteristics of the two ICD's using the 28 rod configuration are shown in Fig. 17. Since this rod configuration produces its calibrating signal primarily at the low forward

angles the ICD comparisons with the baseline should be made at these angles. Fig. 17(a) presents the results for the 10 500 rpm condition. Although the data do not completely agree with the baseline at the low angles ($0^\circ - 40^\circ$), no clear effect of any transmission loss for either ICD is indicated. Fig. 17(b) presents the results for the 13 500 rpm condition. The results here indicate considerable transmission loss for ICD number 2 with a much smaller loss for ICD number 1. It should be pointed out here that the 28 rod data, especially at low inlet angles, was not highly repeatable and thus the apparent small difference in tone level between ICD number 1 and the baseline near the 20° angle may not be transmission loss.

The transmission characteristics for the two ICD's using the 41 rod configuration are presented in Fig. 18. Fig. 18(a) shows the results of the calibration at 8450 rpm fan speed. The data for ICD number 1 agrees very closely with the 41 rod baseline case throughout the region dominated by the 41 rod tone. ICD number 2 also agrees fairly well with the baseline throughout the range of interest (40° to 90°). The results for the 10 500 rpm fan speed case are presented in Fig. 18(b). ICD number 1 again agrees very closely with the baseline indicating no transmission loss or redirection effects. ICD number 2 however appeared to attenuate and redirect the propagating tone over nearly all the far field microphone locations. Fig. 18(c) presents the results at the 13 500 rpm fan speed condition. Again the results at this speed condition indicate no transmission problem with ICD number 1 but ICD number 2 appears to cause transmission loss at most of the far field stations.

In summary the use of the rods to determine the transmission loss characteristics of the ICD's proved valuable. A strong BPF tone was generated which was generally unaffected by the presence of the ICD's and thus any change in the far field noise levels with the ICD's could be attributed to the transmission characteristics of the device. The rod results generally verified that ICD number 1 did not have transmission losses over the entire speed range but that ICD number 2 appeared to cause losses at the highest engine fan speed (13 500 rpm). The results for ICD number 2 at 10 500 rpm however, were less clear in that the 28 rod configuration indicated no losses but the 41 rod configuration did indicate a loss. This result could be explained by the different modal pattern generated by the 41 rods and the ability of the ICD to transmit these modes. However in another example without rods at 10 500 rpm, ICD number 2 produced essentially identical far field BPF tone directivity as ICD number 1 and the modal pattern for this case should have been similar to the 41 rod case. Further analysis of the rod results is given in reference 8.

Concluding Remarks

An evaluation of two inflow control devices was made to determine their ability to remove engine inflow turbulence (as determined by a reduction in fan BPF tone) and to allow unaltered sound transmission of fan noise to the far field. The overall objective of the program was to deter-

mine the extent to which these devices could be used for flight simulation of turbofan engine fan noise on a ground based static engine test stand. The engine used in the investigation was a JT15D engine.

The results generally indicated that both an in-duct ICD and an external duct ICD were effective in reducing the turbulence generated blade passing frequency tone. With the ICD, the tone protruded only about 1/3 as far above the broadband level as it did without the ICD. The residual BPF tone could have in part been caused by the fan rotor wakes interacting with the core stators of the production JT15D engine, a cut-on tone.

The transmission characteristics of the two ICD's were evaluated by use of rods installed upstream of the fan. Two rod configurations were used to generate both axisymmetric modes including the plain wave and spinning mode BPF tones. The two rod configurations generated high BPF tone levels that provided transmission calibrations over a range of far field directivity angles. The internal duct ICD appeared to cause sound transmission losses and changes in far field directivity but the external duct ICD was essentially transparent to the propagating tone.

References

1. Feiler, C. E., and Merriman, J. E., "Effects of Forward Velocity and Acoustic Treatment on Inlet Fan Noise," AIAA Paper 74-946, Aug. 1974.
2. Feiler, C. E., and Groeneweg, J. F., "Summary of Forward Velocity Effects on Fan Noise," AIAA Paper 77-1319, Oct. 1977.
3. Shaw, L. M., Woodward, R. P., Glaser, F. W., and Dastoli, B. J., "Inlet Turbulence and Fan Noise Measurement in an Anechoic Wind Tunnel and Statically with an Inlet Flow Control Device," AIAA Paper 77-1345, Oct. 1977.
4. Woodward, R. P., Wazylniak, J. A., Shaw, L. M., and Mackinnon, M. J., "Effectiveness of an Inlet Flow Turbulence Control Device to Simulate Flight Fan Noise in an Anechoic Chamber," NASA TM-73855, 1977.
5. Hodder, B. K., "An Investigation of Possible Causes for the Reduction of Fan Noise in Flight," AIAA Paper 76-585, July 1976.
6. Smith, E. B., Benzakein, M. J., Radecki, K. P., "Study and Tests to Reduce Compressor Sounds of Jet Aircraft," Federal Aviation Agency, FAA-DS-68-7, Feb. 1968.
7. Burdaall, E. A., and Urban, R. H., "Fan-Compressor Noise: Prediction, Research, and Reduction Studies," Federal Aviation Agency, FAA-RD-71-73, Feb. 1971.
8. Heidmann, M. F., Saule, A. V., and McArdle, J. G., "Analysis of Radiation Patterns of Interaction Tones Generated by Inlet Rods in the JT15D Engine," AIAA Paper 79-0581, Mar. 1979.
9. Montegani, F. J., "Some Propulsion System Noise Data Handling Conventions and Computer Programs Used at the Lewis Research Center," NASA TM X-3013, 1974.

ORIGINAL PAGE IS
OF POOR QUALITY

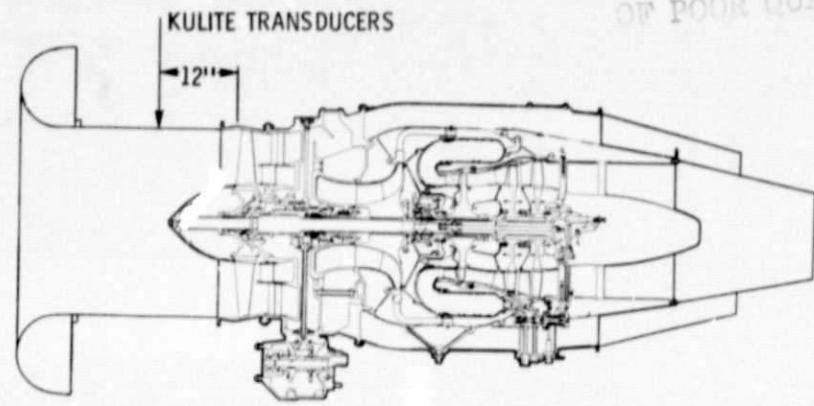


Figure 1. - Cross section view of JT15D engine.

E-9889

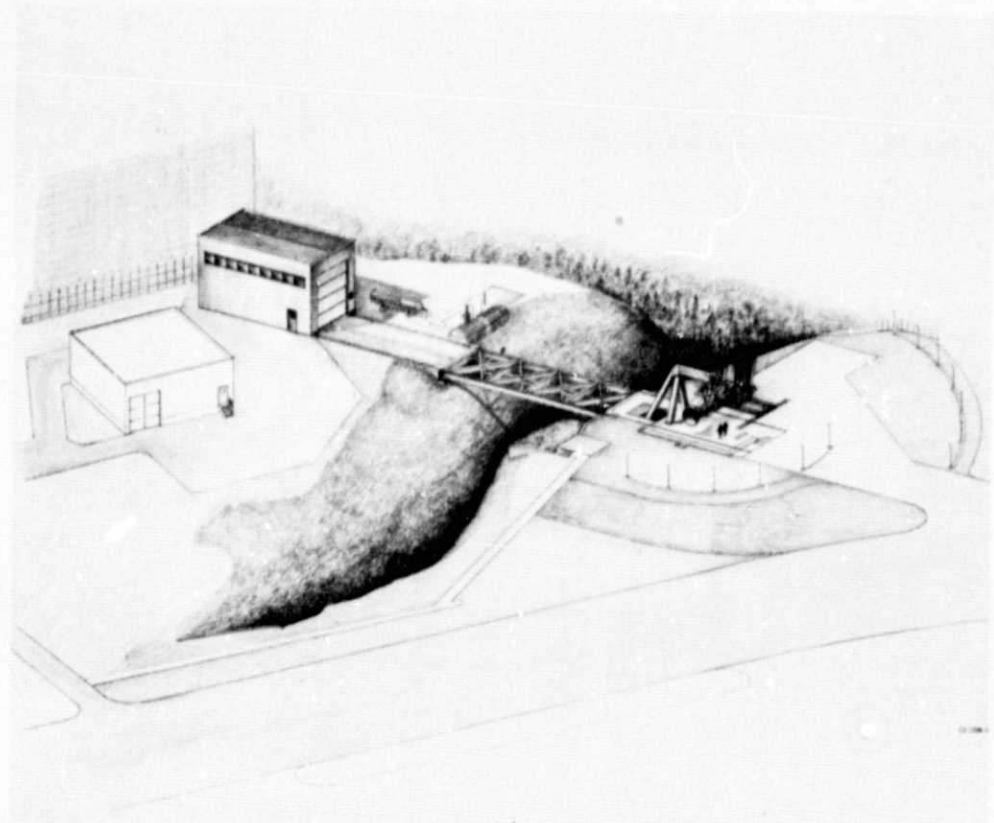


Figure 2. - Perspective illustration of engine test facility.

ORIGINAL PAGE IS
OF POOR QUALITY



Figure 3. - JT15D engine mounted on test stand.

E-9889

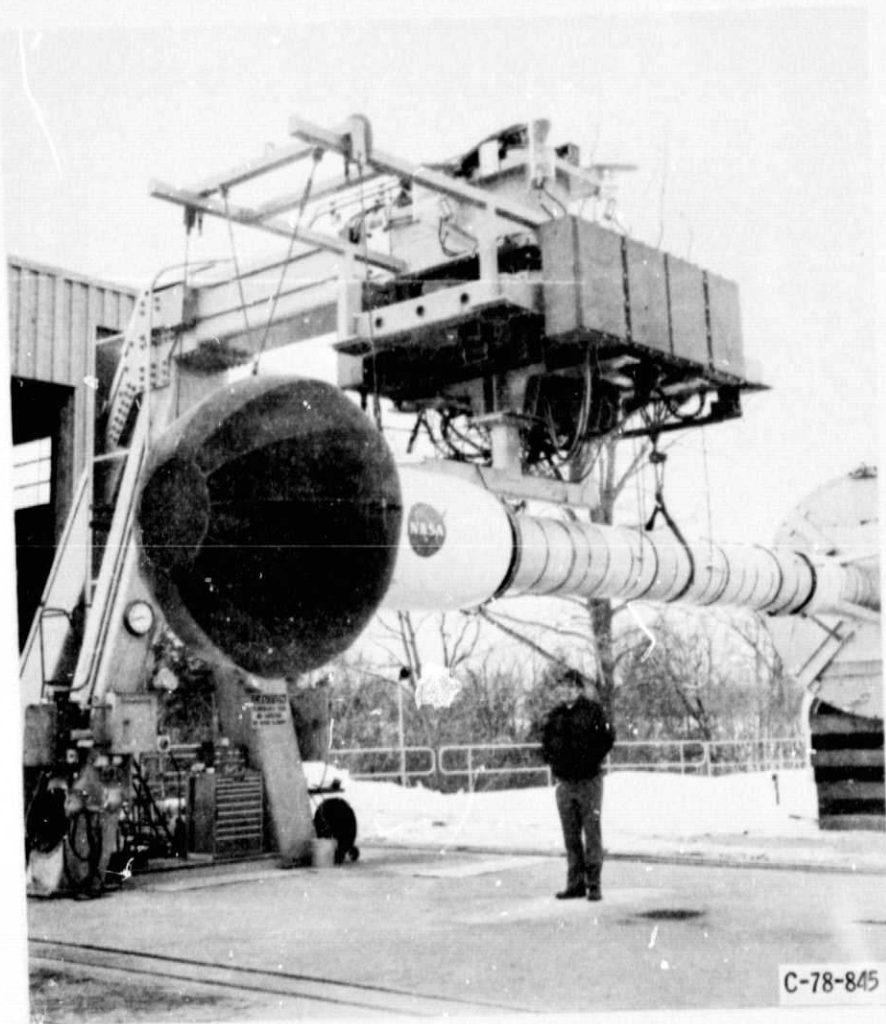


Figure 4. - JT15D engine with external duct ICD mounted to engine.

ORIGINAL PAGE IS
OF POOR QUALITY

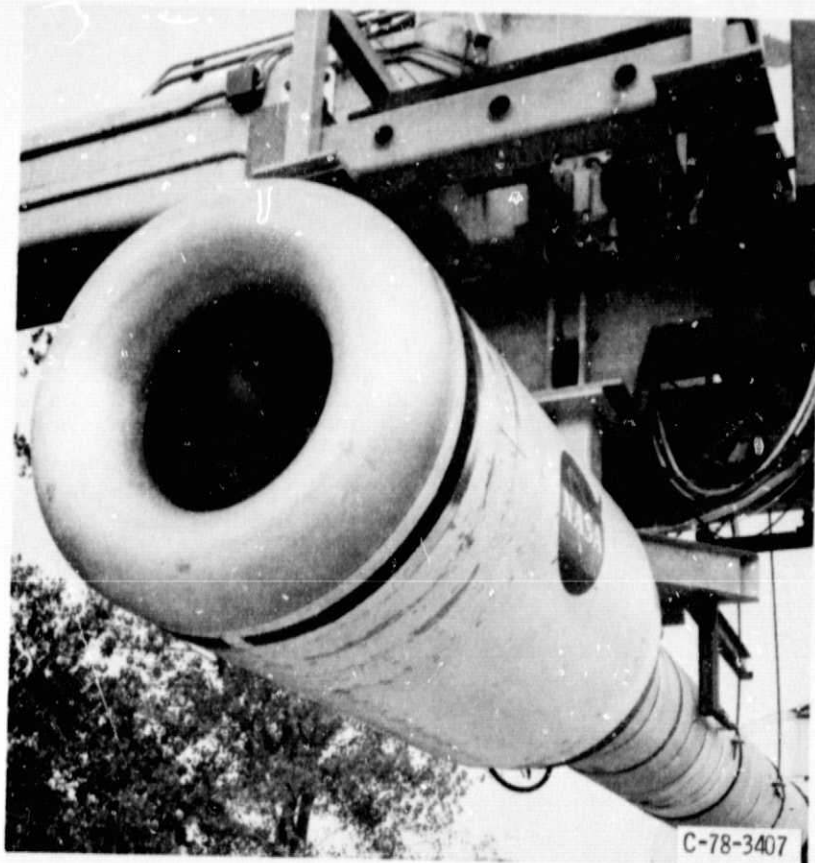


Figure 5. - JT15D engine with internal duct ICD installed.

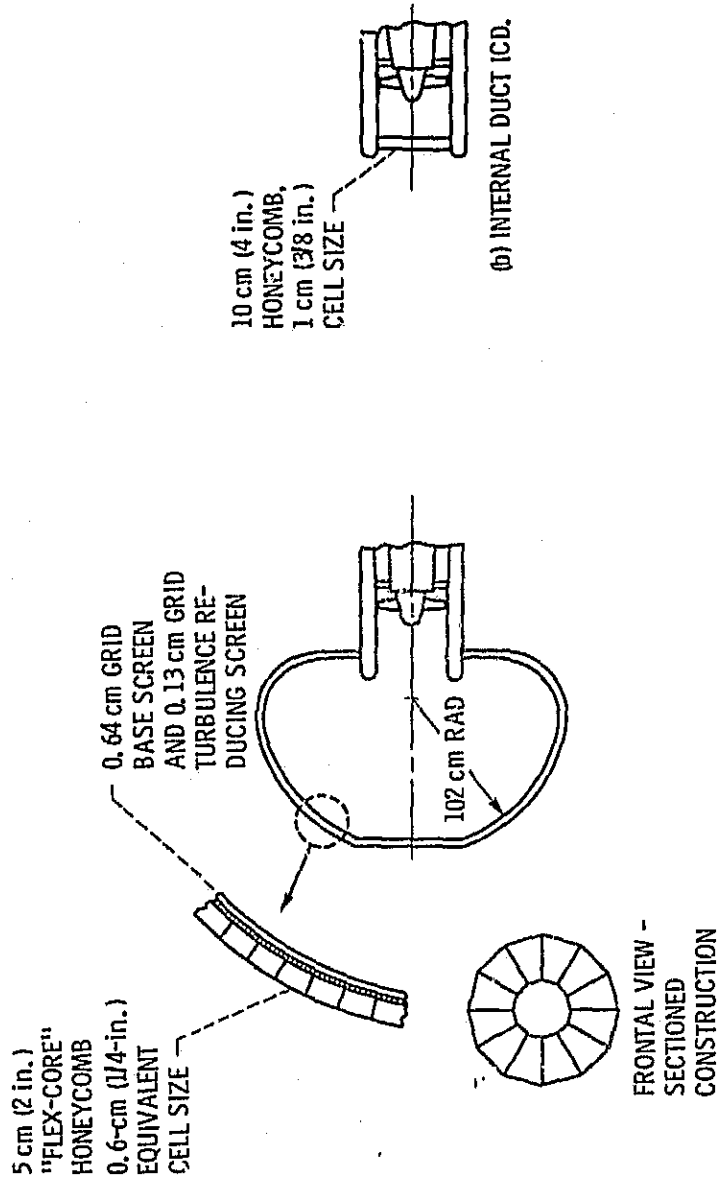
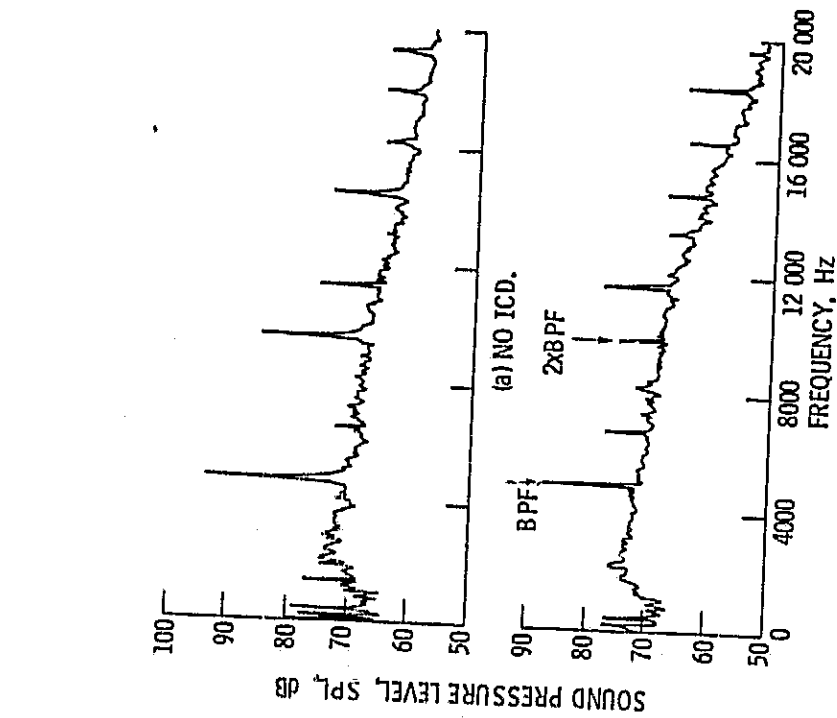
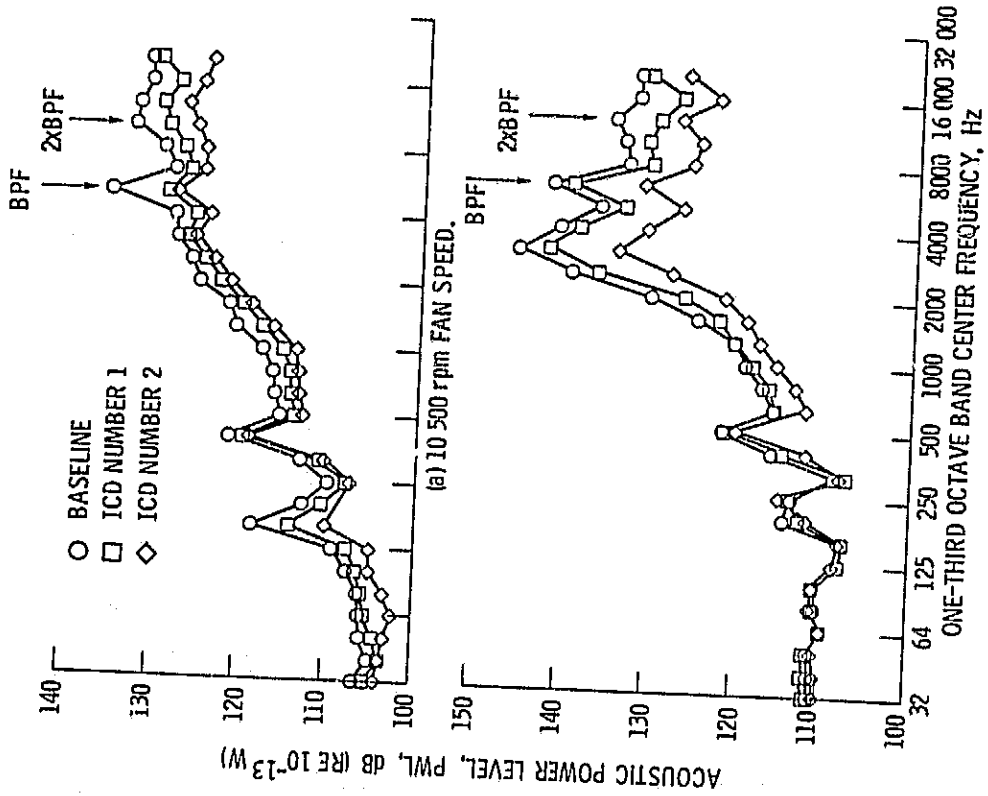


Figure 6. - Schematic sketch of inflow control devices (ICD's) used in tests.



(b) ICD NUMBER 1.

Figure 8. - Narrow-band spectra, 60° far field, 10 500 rpm fan speed.



(b) 13 500 rpm FAN SPEED.

Figure 7. - Power spectra, ICD numbers 1 and 2.

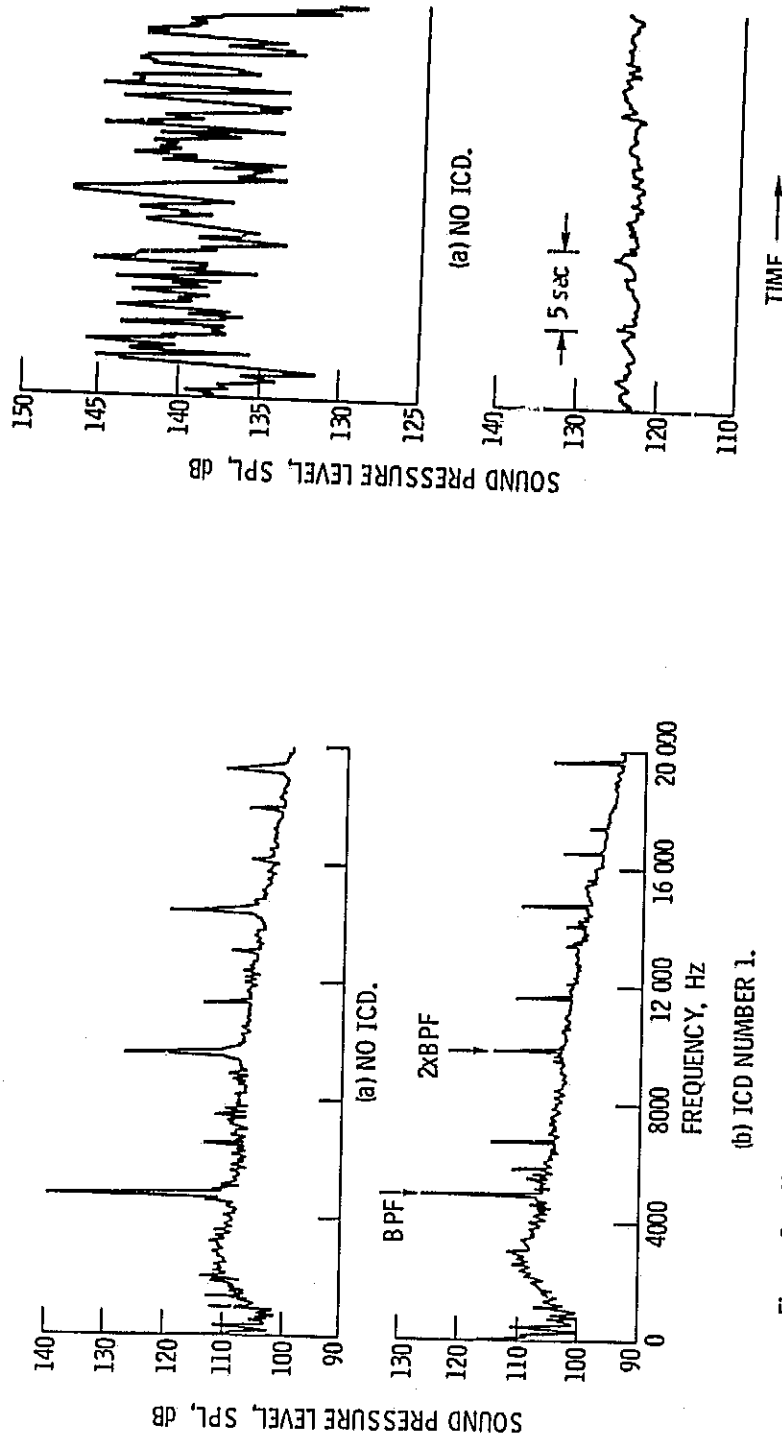


Figure 9. - Narrow-band spectra, in-duct Kulite, 10 500 rpm fan speed.

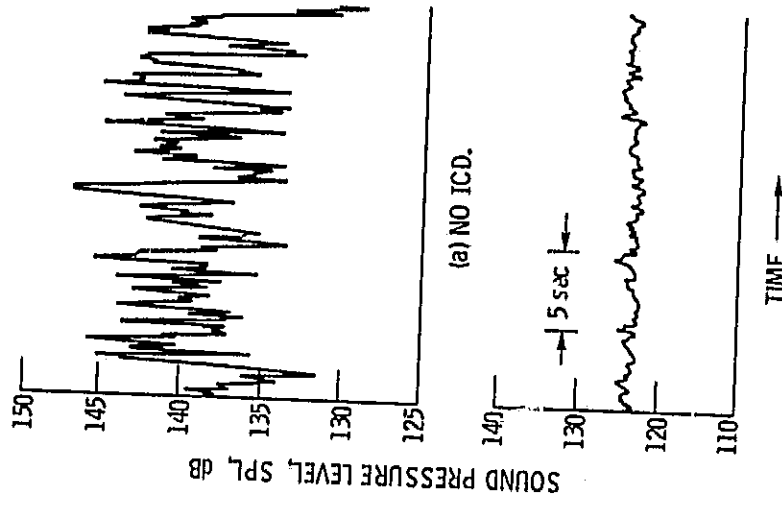


Figure 10. - Time trace, in-duct Kulite, 10 500 rpm fan speed.

ORIGINAL PAGE IS
OF 14

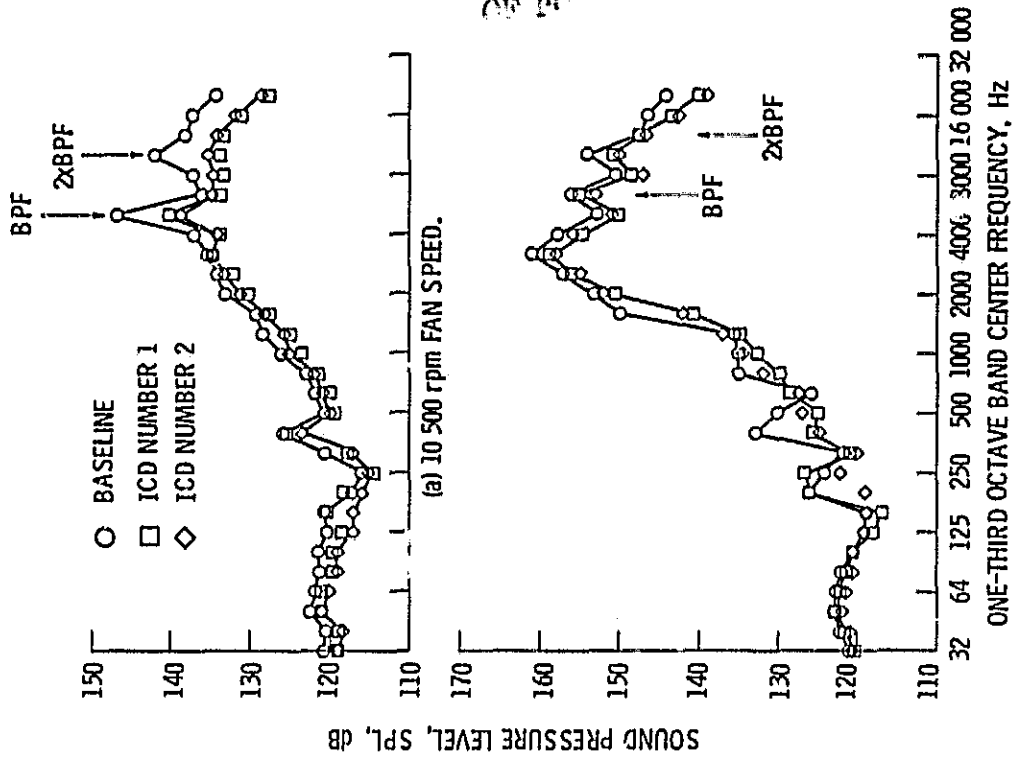


Figure 12. - Sound pressure level spectra, ICD numbers 1 and 2, in-duct Kulfite.
(a) 10 500 rpm FAN SPEED.
(b) 13 500 rpm FAN SPEED.

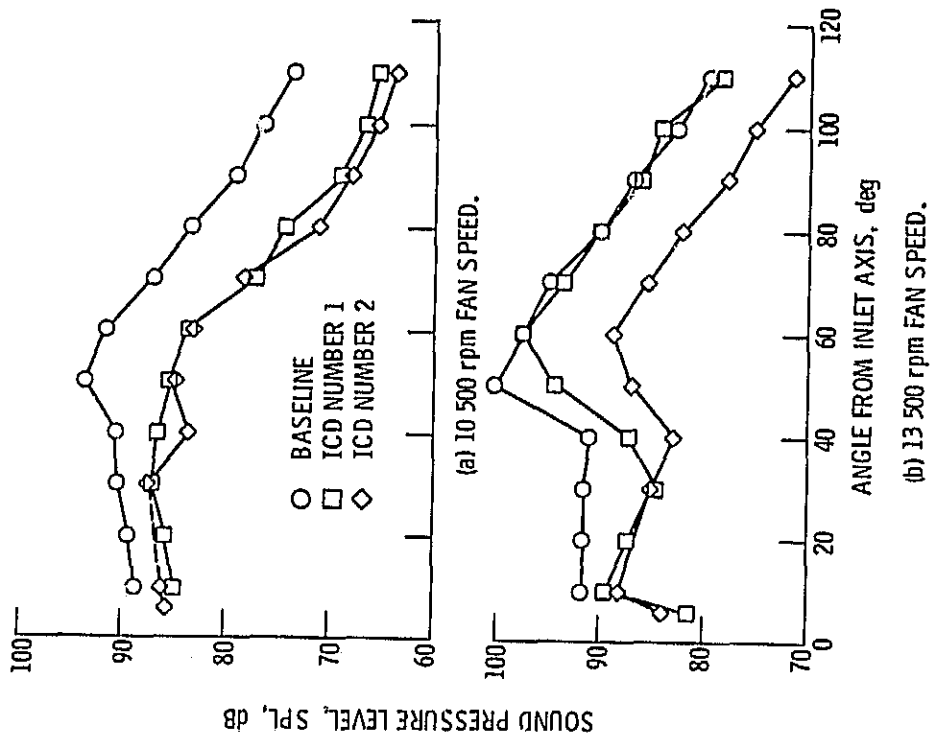


Figure 11. - One-third octave band BPF tone directivity for ICD numbers 1 and 2.
(a) 10 500 rpm FAN SPEED.
(b) 13 500 rpm FAN SPEED.

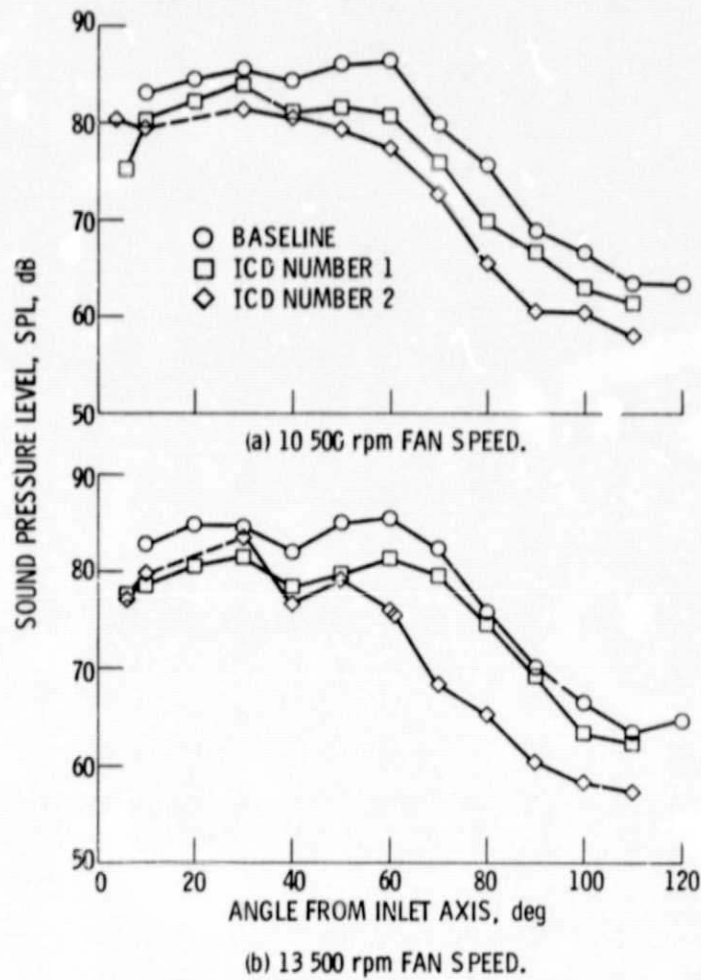


Figure 13. - One-third octave band second harmonic BPF tone directivity for ICD numbers 1 and 2.

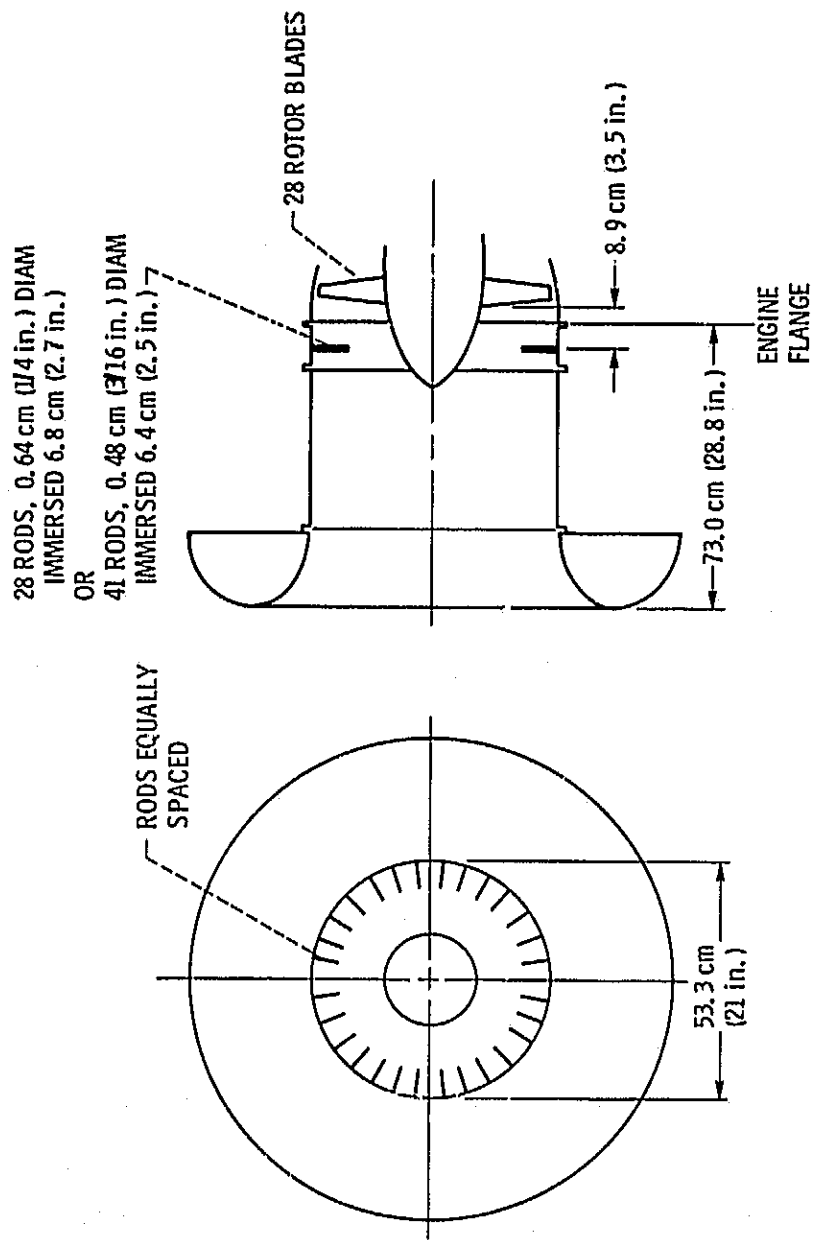


Figure 14. - Schematic diagram of rod installation.

ORIGINAL PAGE IS
OF POOR QUALITY

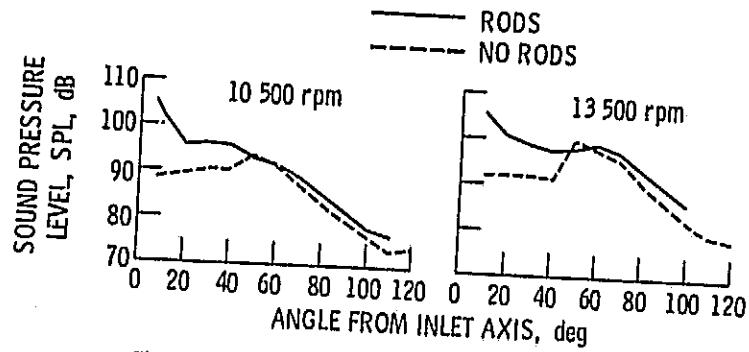


Figure 15. - One-third octave band BPF tone directivity, 28 rod configuration, 10 500 rpm and 13 500 rpm fan speeds.

E-9887

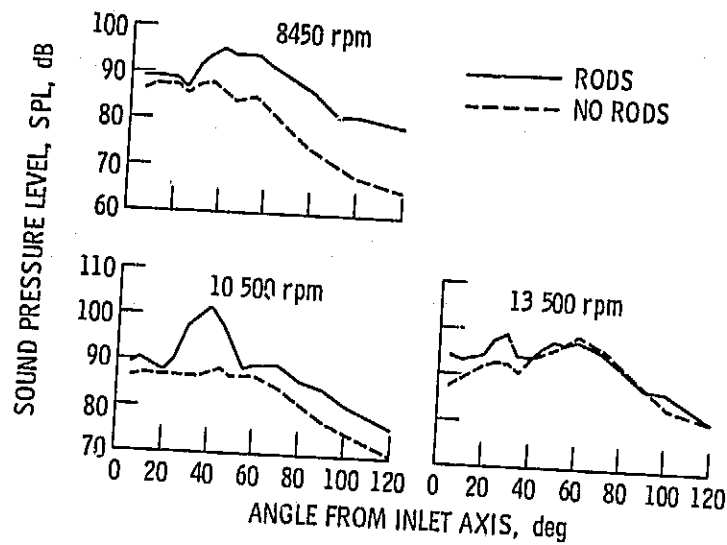
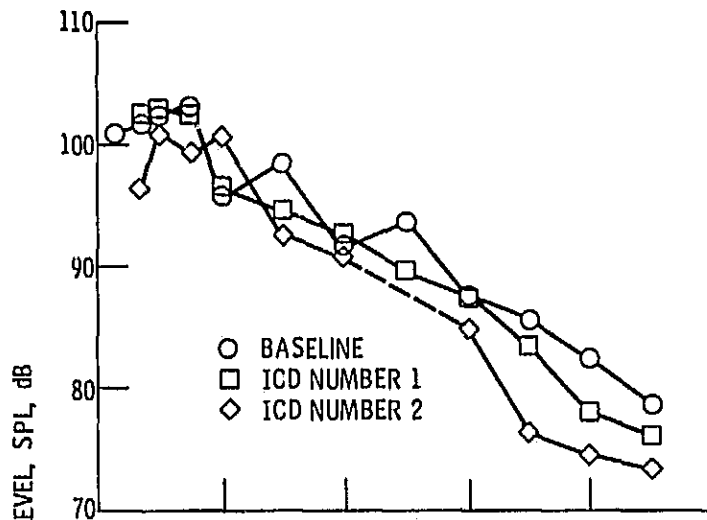
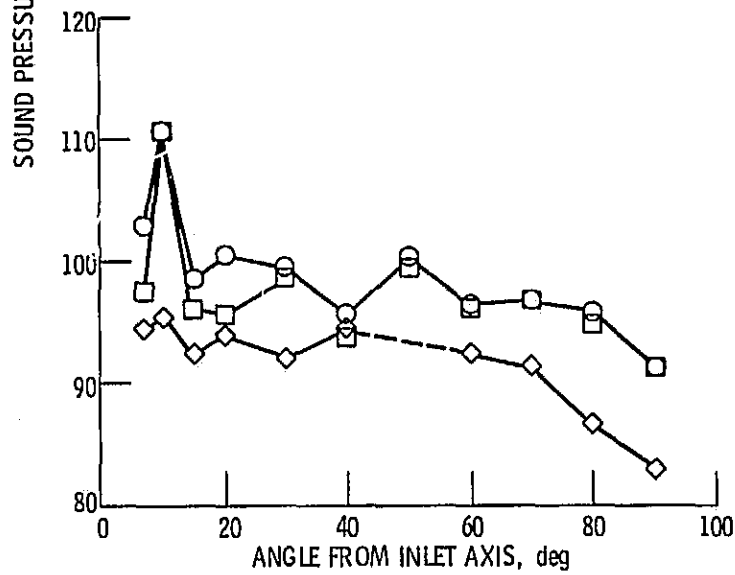


Figure 16. - One-third octave band BPF tone directivity, 41 rod configurations, 8450 rpm, 10 500 rpm, and 13 500 rpm fan speeds.



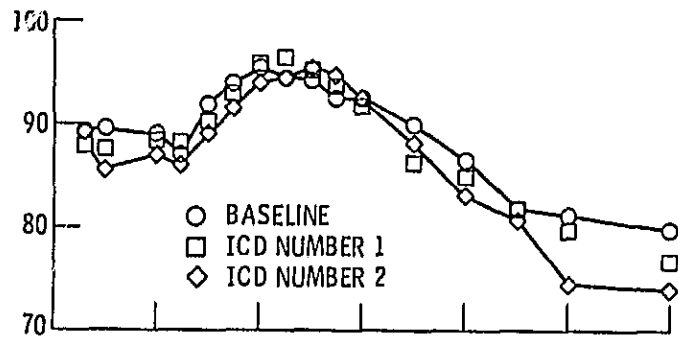
(a) 10 500 rpm FAN SPEED.



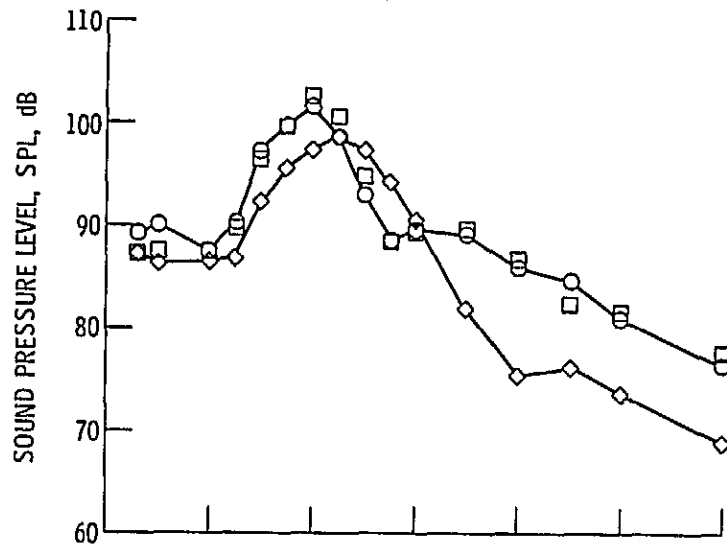
(b) 13 500 rpm FAN SPEED.

Figure 17. - One-third octave band BPF tone directivity for ICD numbers 1 and 2, 28-rod configuration.

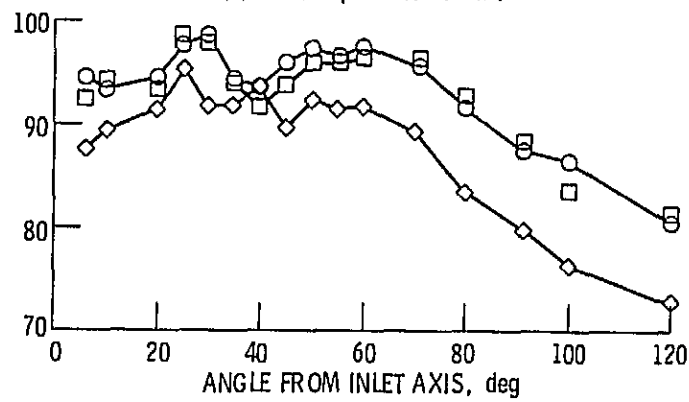
E-9889



(a) 8450 rpm FAN SPEED.



(b) 10500 rpm FAN SPEED.



(c) 13500 rpm FAN SPEED.

Figure 18. - One-third octave band BPF tone directivity for ICD numbers 1 and 2, 41-rod configuration.